Reconfigurable phase-change photomask for grayscale photolithography

Q. Wang[1]*, G. H. Yuan[2]*, K. S. Kiang[3], K. Sun[3], B. Gholipour[4], E. T. F. Rogers[4,5], K. Huang[1], S. S. Ang[1], N. I. Zheludev[2,4] and J. H. Teng[1]

[1]*Institute of Materials Research and Engineering, Agency for Science, Technology and Research (A*STAR), 2 Fusionopolis Way, Innovis, Singapore 138634, Singapore*
[2]*TPI & Centre for Disruptive Photonic Technologies, Nanyang Technological University, Singapore 637371, Singapore*
[3]*Southampton Nanofabrication Centre, Faculty of Physical Sciences and Engineering, University of Southampton, UK, SO17 1BJ*
[4]*Optoelectronics Research Centre and Centre for Photonic Metamaterials, University of Southampton, Highfield, Southampton, SO17 1BJ, UK*
[5]*Instiute for Life Sciences, University of Southampton, Highfield, Southampton, SO17 1BJ, UK*

We demonstrate a grayscale photolithography technique which uses a thin phase-change film as a photomask to locally control the exposure dose and allows three-dimensional (3D) sculpting photoresist for the manufacture of 3D structures. Unlike traditional photomasks, the transmission of the phase-change material photomask can be set to an arbitrary gray level with submicron lateral resolution, and the mask pattern can be optically reconfigured on demand, by inducing a refractive-index-changing phase-transition with femtosecond laser pulses. We show a spiral phase plate and a phase-type super-oscillatory lens fabricated on Si wafers to demonstrate the range of applications that can be addressed with this technique.

*These authors contributed equally to this work.

1 Introduction

Photolithography is a well-established manufacturing technique for electronic, optical, and microelectromechanical system (MEMS) applications[11111]. The standard process consists of: manufacture of a mask containing transparent/opaque features; UV exposure through the mask to transfer the pattern onto a thin layer of photoresist; and development of the photoresist to form the pattern either in the resist itself or a layer of material beneath the resist. In the traditional photolithography, a binary (two-level) photomask is used, allowing creation of two-dimensional (2D) patterns in the photoresist, but with uniform height. Three-dimensional (3D) fabrication normally requires multiple photolithography and alignment processes, which is both time consuming and technically challenging. In light of this, grayscale lithography mask is a very attractive proposition, allowing fast-turnaround, 3D microdevice prototyping.

In the past few years, there have been many advances in grayscale mask design and lithography process. Gray-tone lithography is based on a dithering process: using conventional quartz/Cr masks with plurality of sub-resolution transparent openings, or based on photo-emulsion film with a varying the density of silver grains, to modulate the ultraviolet light intensity [2] [3] [4]. Since the transmittance of a gray level in gray-tone mask is determined by the ratio of the number of opaque spots to clear spots within a grayscale element, the lateral resolution is limited to a few micrometers.

High-energy-beam sensitive (HEBS) glass masks selectively change metal-ion concentration on exposure to electron beams, resulting in transparency differences and allowing the manufacture of grayscale masks[5]. Other 3D micro-fabrication methods include using microfluidic photomasks[6] or a polymer photomask doped with laser dye[7]. Those techniques are not in widespread use in either industry or academic laboratories because they are either restricted to a limited range of shapes or not scalable to large-scale processing. Grayscale photomasks created by direct laser writing in metallic thin films can also achieve continuous-tone gray levels [8] [9]. However, the photomask usually has a fixed pattern once fabricated and changing the design requires the fabrication of a completely new mask. In this work, we demonstrate a reconfigurable, submicron-resolution grayscale photolithography mask based on a phase-change ultrathin film. This combines the advantages of direct laser writing and 3D printing technologies – it can be flexibly modified to correct errors or iteratively improve the design with those of conventional lithography – the final mask can be used repeatedly in batch production.

The photomask is made from the phase change material $Ge_2Sb_2Te_5$ (GST), which has been widely used in optical data storage and non-volatile memory because of its large change in optical/electronic properties between the amorphous and crystalline states[10] [11] [12]. We use a series of low-energy femtosecond (fs) laser pulses to gradually change the complex refractive index of the film by partially crystallizing the (initially amorphous) film at a particular point[13] [14] [15]. In contrast to previous works using nanosecond laser pulses, we use lower-fluence fs laser pulses to change the phase of the film, resulting in a sharper border between the amorphous background and the crystallized spots, giving a smaller mark footprint and finer pattern features[13] [16]. The grayscale pattern can then be transferred into a silicon wafer with a one-step photolithography process, using GST grayscale pattern as the mask, followed by a reactive ion etching process to create multi-height pattern. The reversible phase change in the GST film allows erasing and reconfiguration of the patterns after writing[17] [18], which is highly beneficial in situations where the photomask is being iteratively deigned: for example in a scheme where the process recipe is still under development, or the precise device design needs to be tested and adjusted.

2 Experimental procedure and results

In our experiments, a three-layer phase-change "canvas", which comprises of a 70 nm thick amorphous GST layer sandwiched between two 70 nm thick ZnS-SiO_2 protective layers was deposited on a silica substrate by sputtering. A 730 nm, 75 fs pulse train was reduced to 1 MHz frequency using an electro-optical modulator and focused onto a GST film. To write a pattern in the GST, a low pulse energy was used to heat the film below the melting point but above the glass-transition temperature and thus gradually crystallize it[13]. The size and contrast of crystallized mark can be precisely controlled by selecting the pulse energy and number of pulses used. To erase the mark, a single high-energy pulse was applied to have the GST mark melted and cooled rapidly to form the amorphous phase[13].

Using this writing mechanism, we can create reconfigurable binary and grayscale GST photomasks for optical lithography. To demonstrate the technique, we manufactured a 3D spiral phase plate (SPP). These plates are used in many systems to convert a Gaussian beam into a "doughnut" beam – as used in, for example, stimulated emission depletion microscopy[19] – or to impart orbital angular momentum to a light beam[20]. The spiral plate has an increasing thickness in the azimuthal direction, imparting a phase that varies as a function of angle, but is constant over the radius of the beam. SPPs are normally fabricated by multi-step photolithography and etching[21], or direct electron beam writing[22]. With our proposed multi-level grayscale lithography, we can create the 3D silicon structure with one lithography and etching step.

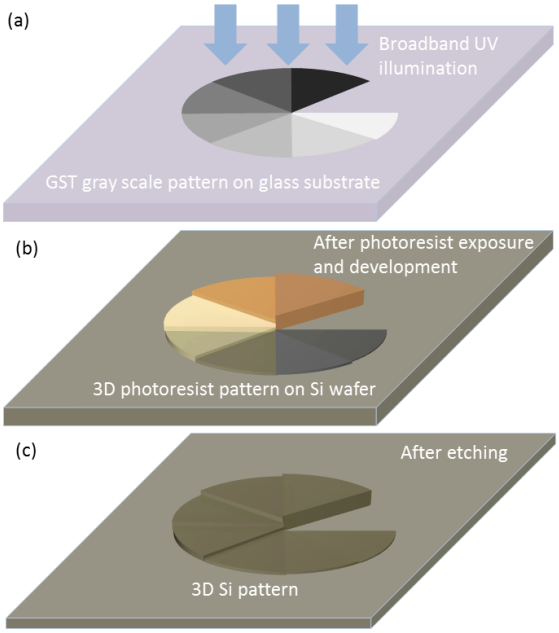

FIG. 1. Sketch of the 3D spiral phase plate fabrication process. (a) Grayscale photomask is prepared by direct optical writing in a GST thin film. (b) The photoresist is exposed and developed leaving a 3D photoresist structure on the substrate. (c) 3D silicon structure is obtained by uniform etching of the substrate and remaining photoresist.

Figure 1 shows a schematic of the 3D optical lithography fabrication process. When a positive photoresist is exposed to UV light, polymer-chain-breaking in the exposed areas makes them more soluble in the photoresist developer: the photoresist is initially hard and is then softened by exposure. Crucially, this softening happens progressively from the top of the photoresist layer to the bottom. A low dose will expose (soften) only the top of the layer, while a high dose will expose the whole layer. When a GST pattern is used as a photomask, differing transmission through the different gray levels of the pattern means that the exposure dose is varied, resulting in different depths of exposed photoresist across the surface. A solvent is used to wash away the soft parts on the surface, leaving unexposed underlying photoresist which forms a 3D structure. In our experiments, the positive photoresist AZ1505 was spin coated at 4000 RPM on the clean silicon wafer and then soft baked on hotplate for 1 minute, giving a resist thickness of ~0.5 μm. The resist was exposed in a Mask Aligner (Karl Suss Mask Aligner-MA6) using i-line (intensity 19mW/cm^2)

with a broadband exposure of 120 seconds. After development, a variable thickness photoresist is left on the silicon wafer to be used as the etching mask. When the etching is complete, the desired 3D pattern is left standing on the Si wafer. Due to the high UV absorption of GST compared to a standard mask substrate[23], a longer exposure time is required and its optimization would increase the attractiveness of our grayscale lithography process.

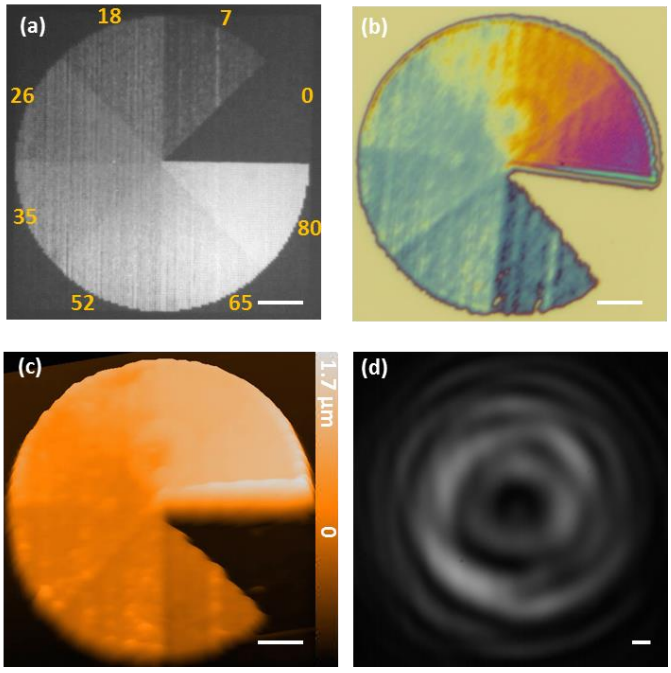

FIG. 2. Manufacturing a 3D Si structure using grayscale lithography. (a) Reflection microscope image of 8 level grayscale pattern written into a GST thin film. The number of pulses used to write each grayscale section is indicated in the figure. (b) Color microscope image of 3D photoresist structure on Si wafer after photolithography and resist development. Color is due to thin film reflection. (c) Surface profiler characterization of the 3D SPP pattern with each section a different thickness. Color shows surface height on a scale from 0 to 1.7μm. (d) The image of optical vortex (1 mm away from the sample) generated by the SPP with illumination of a Gaussian beam (λ=1.6 μm) through the substrate. Scale bar: 10 μm.

Figure 2a shows an 8-level grayscale circularly ramped pattern written in GST where each mark was written with a controlled number of pulses between 0 and 80. The partially crystallized GST formed a grayscale mark with both a mark size and a pixel pitch of 0.59 μm. Figure 2b shows an optical micrograph of a 3D photoresist pattern after development. The color of the pattern was due to the interference of light reflected from the top and bottom surfaces of the photoresist. There were 8 different colors, corresponding to 8 different thicknesses of photoresist (and the 8 gray levels in the mask). The pattern was transferred into the silicon substrate by inductively coupled plasma (ICP) etching (Oxford PlasmaPro 80plus system). The 3D photoresist pattern protected the Si substrate from the plasma etching until it was etched away: larger heights of photoresist gave more amounts of protection and hence less etch depths in the silicon. After etching, the photoresist had been completely removed, leaving the multi-height pattern etched onto the Si wafer.

Figure 2c shows the surface profiler image of 3D SPP pattern on Si with 8 sectors of different heights. The sectors of SPP gradually increased in height from 0 to 1.7 μm, in the clockwise direction. Thus, the phase distribution of the laser beam passing through the SPP had a total spiral phase change of $2.55\times2\pi$ around the optical axis. Figure 2d demonstrates the observed optical vortex image of the SPP illuminated by a focused Gaussian beam (λ=1.6 μm) through the substrate. The dark area in the center of the image revealed the generation of an on-axis optical phase singularity. The non-uniform ring shape optical vortex pattern was because of the non-integer topological charge induced by SPP [24], and diffraction from the rough surface and the edge of the pattern.

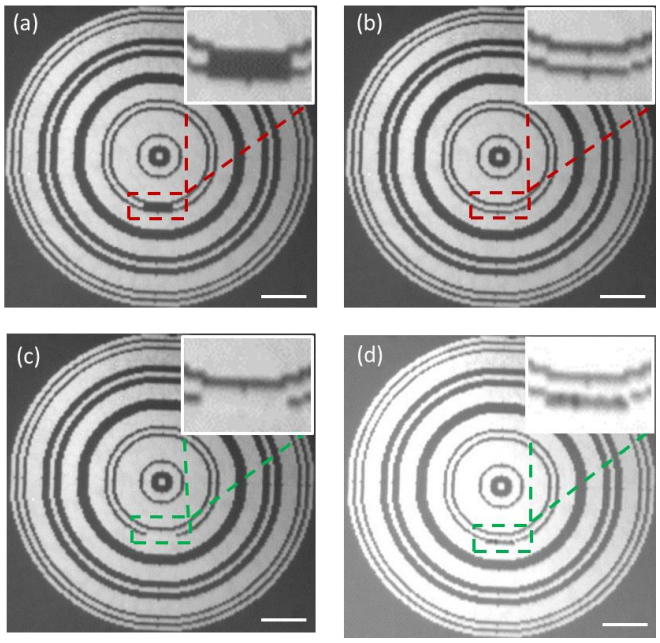

FIG. 3. Reconfiguration of a photomask on a GST film. (a) Optical micrograph of the written photomask with a deliberate defect: one crystallized line is missing. (b) The defect was subsequently corrected with another writing procedure crystallizing only the missing line. (c) Optical micrograph of a written photomask with a defect of on extra crystallized region (15×1 pixels). (d) The defect was corrected by re-amorphization of the GST marks one by one. Scale bar: 10 μm.

One of the major advantages of using a phase change material as the photomask layer is its capability to correct mask errors, or modify a written mask if it does not work as desired, using its reversibly switchable phase states, as demonstrated in Fig 3. We design and write photomask pattern (121×121 pixels) with a deliberate defect using trains of 80 laser pulses (pulse energy ~0.39 nJ) per point (Fig 3a). Afterwards, the photomask defect was corrected by using fs pulse trains with same conditions to crystallize the GST film (Fig 3b) at the missing points. For defects where there are too many crystallized GST marks, such as the one shown in Fig 3c with an extra crystalline section, we can correct the defect using a single fs pulse with high energy (~1.25 nJ) to re-amorphize GST marks (Fig 3d).

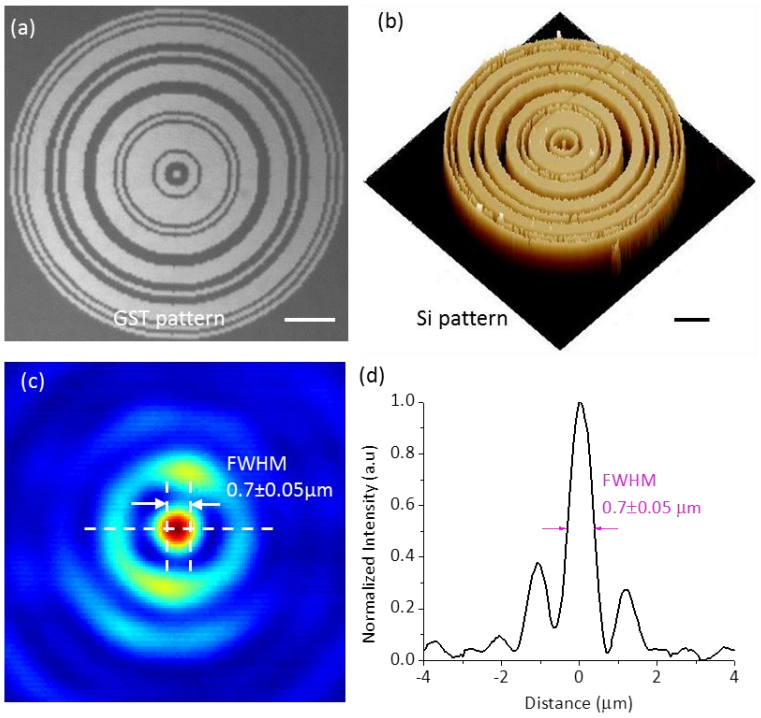

FIG. 4. Optical lithography of an sub-diffraction-limited focusing SOL in Si. (a) Reflection microscope image of the SOL in GST (photomask). (b) AFM image of the two-step phase SOL etched in a Si wafer. The etch depth is 318±5 nm. (c) Focused hotspot from the SOL at 1550 nm wavelength. (d) The cross section of SOL hotspot image shows the FWHM size is 0.7 μm (0.45 λ). Scale bar in (a) and (b): 10 μm.

In our experiments, the finest photomask structure is primarily determined by the size of each GST mark, and hence can be used for submicron scale optical lithography. Here, we also demonstrate the direct optical writing of a high resolution photomask for the fabrication of a two-step phase super-oscillatory lens (SOL) in silicon. The SOL is a device capable of sub-diffraction-limited focusing of light [25], and is here designed for operation at wavelength of 1550 nm. The SOL is composed of a sequence of concentric rings whose width and diameter are intricately designed to produce a focal spot with the required properties[26]. Interference of the waves transmitted through the SOL leads to a complex diffraction pattern with subwavelength hotspot at the center. Compared with a traditional amplitude based SOL (with alternating opaque and transparent rings), the phase-type SOL has all of its rings transparent (but with π phase shift to produce the interference) to enhance the focusing efficiency. The smallest ring width (feature size) in our design is 0.89 μm, which is two of our GST marks, as demonstrated in Fig 4 a. The mark space in this design is decreased to 0.445 μm in order to partially overlap of marks for achieving the uniform photomask pattern. We used positive photoresist AZ701 for the SOL fabrication as it is capable of submicron resolution lithography. It was spin-coated on the Si wafer with a thickness of 700 nm and soft baked for 1 min to remove the solvent. After UV exposure for 58s (intensity 18 mW/cm^2) with the GST photomask and photoresist development, the SOL pattern was recorded in the photoresist. The pattern was then transferred to the Si wafer using an ICP system (OIPT PlasmaPro 100 Cobra) etching to a depth of 318±5 nm, which introduces π phase shift for 1550 nm light, as designed.

The phase SOL was characterized under an optical microscope with a high numerical aperture objective lens (Nikon CFI LU Plan Apo EPI 150×) and an additional 4 times magnification imaging system (Magnification changer: Nikon C-Mount TV Adaptor VM 4×) in order to record both high spatial frequency information and subwavelength features on a high-resolution sCMOS camera (Andor Neo, 2560×2160). Figures 4c and 4d show the FWHM of the SOL hotspot generated at a distance of 20 μm is 0.7 μm, corresponding to 0.45 λ, which is below the diffraction limit of 0.5 λ. Previously, SOLs have been fabricated only using electron beam lithography or focused ion beam milling in metal thin film[26 27]. In this report, the phase type SOL is fabricated by one optical lithographic step, thus enabling batch manufacture for large-scale production. Although only two-step phase SOL is introduced here, such lithography technique can be extended into multi-level phase-type SOL after appropriately controlling the exposure parameters of the GST photomasks and photoresists.

3 Conclusions

In summary, we report reconfigurable, submicron-resolution grayscale lithography masks based on nanometer thick phase-change thin films. The grayscale mask was prepared by direct optical writing on the phase change GST film using fs laser pulse trains to gradually and locally crystallize the GST. We first used a one-step grayscale lithography process with our optically written mask to fabricate a silicon pattern with 8 discrete heights suitable for use as an optical vortex generator. A reconfigurable photomask was then conceptually demonstrated, where defects can be corrected after the writing process. Additionally, we fabricated a silicon based phase-type super-oscillatory lens which has submicron lateral feature size and is capable of sub-diffraction-limited focusing. One-step photolithography for 3D patterning, with sub-micron feature size and pattern-reconfiguration and error-correction capability, is very promising for a range of application, such as diffractive optical elements, blazed gratings, integrated photonics circuits and MEMS systems.

Acknowledgments:
This work was supported by the Engineering and Physical Sciences Research Council [grants EP/F040644/1, EP/M009122/1], the Singapore Ministry of Education [grant MOE2011-T3-1-005], and the Singapore Agency for Science, Technology and Research (A*STAR) [Grants 1521480031, 1527000014 and 1223600009].

Reference:

1 M. J. Madou, Fundamentals of Microfabrication (CRC, Boca Raton, FL) (1997).
2 U.S. Patent 2004/0009413 A1 (15 Jan 2004) T. E. Lizotte.
3 M. Christophersen and B. F. Phlips, Appl. Phys. Lett. **92**, 194102 (2008).
4 W. Henke, W. Hoppe, H. J. Quenzer, P. Staude-Fischbach, and B. Wagner, Jpn. J. Appl. Phys. **33**, 6809 (1994).
5 L. A. Wu C.-K. Wu, U.S. patent 2003/6562523 B1 (13 May 2003).
6 C. Chen, D. hirdes, and A. Foich, PNAS **100** (4), 1499 (2002).
7 N. S. Korivi, Y. X. Zhou, and L. Jiang, J. Vac. Sci. Tech. B **26**, 62 (2008).
8 Chuan Fei Guo, Sihai Cao, Peng Jiang, Ying Fang, Jianming Zhang, Yongtao Fan, Yongsheng Wang, Wendong Xu, Zhensheng Zhao, and Qian Liu, Opt. Express **17**, 19981 (2009).

[9] Chuan Fei Guo, Jianming Zhang, Junjie Miao, Yongtao Fan, and Qian Liu, Opt. Express **18**, 2621 (2010).
[10] M. Mansuripur, Critical Technologies for the Future of Computing **4109**, 162 (2000).
[11] M. H. R. Lankhorst, B. W. S. M. M. Ketelaars, and R. A. M. Wolters, Nat. Mater. **4**, 347 (2005).
[12] Jianzheng Li, Lirong Zheng, Hongzhu Xi, Dingxin Liu, Hongguang Zhang, Ye Tian, Yong Xie, Xing Zhu, and Qian Liu, Phys. Chem. Chem. Phys. **16**, 22281 (2014).
[13] Q. Wang, J. Maddock, E. T. F. Rogers, T. Roy, C. Craig, K. F. Macdonald, D. W. Hewak, and N. I. Zheludev, Appl. Phys. Lett. **104**, 121105 (2014).
[14] J. Hegedus and S. R. Elliott, Nat Mater **7** (5), 399 (2008).
[15] L. P. Shi, T. C. Chong, P. K. Tan, X. S. Miao, Y. M. Huang, and R. Zhao, Jpn. J. Appl. Phys. **38** (3B), 1645 (1999).
[16] W. Zhu, Y. Lu, S. Li, Z. Song, and T. Lai, Opt. Express **20** (17), 18585 (2012).
[17] Q. Wang, E. T. F. Rogers, B. Gholipour, C.-M. Wang, G. H. Yuan, J. H. Teng, and N. I. Zheludev, Nat. Photonics **10**, 60 (2016).
[18] C. D. Wright, Y. Liu, K. I. Kohary, M. M. Aziz, and R. J. Hicken, Adv. Mater. **23**, 3408 (2011).
[19] D. Wildanger, E. Rittweger, L. Kastrup, and S. W. Hell, Opt. Express **16** (13), 9614 (2008).
[20] M. W. Beijersbergen, R. P. C. Coerwinkel, M. Kristensen, and J. P. Woerdman, Opt. Commun **112**, 321 (1994).
[21] S. S. Oemrawsingh, J. A. van Houwelingen, E. R. Eliel, J. P. Woerdman, E. J. Verstegen, J. G. Kloosterboer, and G. W. Hooft, Appl. Opt. **43** (3), 688 (2004).
[22] W. C. Cheong, W. M. Lee, X.-C. Yuan, L.-S. Zhang, K. Dholakia, and H. Wang, Appl. Phys. Lett. **85**, 5784 (2004).
[23] B. S. Lee, J. R. Abelson, S. G. Bishop, D. H. Kang, B. k. Cheong, and K. B. Kim, J. Appl. Phys. **97**, 093509 (2005).
[24] E. Brasselet, G. Gervinskas, G. Seniutinas, and S. juodkazis, Phy. Rev. Lett. **111**, 193901 (2013).
[25] E. T. F. Rogers and N. I. Zheludev, J. Opt. **15**, 094008 (2013).
[26] G. Yuan, E. T. F. Rogers, T. Roy, G. Adamo, Z. Shen, and N. I. Zheludev, Sci. Rep. **4**, 63333 (2014).
[27] E. T. Rogers, J. Lindberg, T. Roy, S. Savo, J. E. Chad, M. R. Dennis, and N. I. Zheludev, Nat. Mater. **11** (5), 432 (2012).